Effect of Sc Addition on Magnetic and Optical Properties of YFeO$_3$ Nano Particles

Meng Wang*

[1] *School of Mechanical and Electrical Engineering, Shenzhen Polytechnic, Shenzhen 518055, China*

Multiferroic Sc-doped YFeO$_3$ nanoparticles were obtained by a low-temperature solid-state reaction route. It indicated that with the addition of Sc, nanosized YFeO$_3$ powders were obtained at 800 ^{o}C, and the orthorhombic phase was transformed into the hexagonal structure. Magnetic hysteresis loop illustrated the magnetic property of YFeO$_3$ nanoparticles improved with Sc doping. The maximum magnetization of the powders was about 4.00 emu/g, showing that the energy gap can be reduced to 2.25 eV and thus the doping nanoparticles can be used in optical field. Therefore, the optical and magnetic properties of the material can be obviously enhanced with Sc doping, proving its potential application in magnetic and optical fields.

Keywords : low-temperature solid-state reaction, optical properties, magnetic properties, Sc addition, YFeO$_3$

1. Introduction

Multiferroic ceramics combine a number of ferroic orders [1, 2]. A few materials have both ferroelectric and ferromagnetic properties simultaneously in nature, as both empty and partially filled d-orbits are required to realize both properties. Both properties are naturally exclusive [3]. These materials can be applied in high storage systems [4, 5]. Among them, the perovskite-type YFeO$_3$ exhibits ferroelectric ordering below −256 °C and antiferromagnetic ordering at high temperature of around 370 °C [6]. Moreover, many studies have been conducted on its atomic ferroelectricity and magnetic properties [7-10]. It has a small optical band gap (around 2.58 eV), making it a good candidate in optical application [11]. There are many methods to fabricate YFeO$_3$ nanoparticles, such as conventional sintering method and sol-gel method. A new method-low-temperature solid-state reaction has been developed [6]. This method only needs to grind by hand, and it possesses the priority of high pure phase and ultrafine grain size. However, an essential problem is yet to control: YFeO$_3$ has two structures, the hexagonal one at low temperature and the orthorhombic one at high temperature. The former one possesses excellent optical properties and the latter one owns a higher magnetic value.

How to combine the priorities of both is an interesting topic for the fabrication and development of YFeO$_3$.

In our work, the Sc^{3+}-doped YFeO$_3$ nanoparticles via low-temperature solid state reaction were introduced. Sc^{3+} can be used to diminish the leakage current of YFeO$_3$ because it possesses a stable electronic structure [12]. In addition, Sc has different ionic radius from Fe, so it can control the transition of the hexagonal and orthorhombic structure of YFeO$_3$, which should be a better way to adjust the magnetic and optical properties. The purpose of this article is to improve both optical and magnetic properties.

In this paper, the Sc-doped YFeO$_3$ nanoparticles were fabricated via the low-temperature solid-state route, and the impact of doping amount was studied. In addition, properties of synthesized YFeO$_3$ nanoparticles were investigated.

2. Experimental

YFeO$_3$ and YFe$_{1-x}$Sc$_x$O$_3$ nanoparticles were harvested by the low-temperature solid-state route, which was elaborated in Ref [6]. First, weighed quantities of Fe (NO$_3$)$_3$·9H$_2$O, Y(NO$_3$)$_3$·6H$_2$O, Sc (NO$_3$)$_3$, and citric acid were mixed and grinded for half an hour. Then the obtained powders were heated for 2 hours at 100 °C to obtain the precursor. After that, the precursor was grinded again and calcined for 2 hours at 900 ^{o}C to obtain

*Corresponding author: Tel: +86-18565873580
Fax: +86-18565873580, e-mail: wangmeng04@szpt.edu.cn

Sc-doped $YFeO_3$ nanopowders. Thus, $YFe_{0.98}Sc_{0.02}O_3$, $YFe_{0.95}Sc_{0.05}O_3$, and $YFe_{0.9}Sc_{0.1}O_3$ nanopaticles were made. The calcined particles were tested by XRD (XRD, D/max-RB, Rigaku, Japan) and SEM (S-4700, Hitachi, Japan). Raman spectra were measured at room temperature by Renishaw InVia Reflex (U.K.) spectrometer, with a range of 100 cm^{-1} to 1500 cm^{-1}. Magnetic hysteresis loops were measured by PPMS (PPMS, QUANTUM DESIGN, DynaCool-9T) at room temperature and optical absorbance properties of powders were studied by UV-Visible spectrophotometer (SHIMADZU, UV-2600).

3. Results and Discussion

Figure 1 illustrates the XRD patterns of the obtained nanoparticles. As it shows, the formation of the phase of the particles were decided by the Sc addition amount. The pattern of $YFeO_3$ phase of $YFe_{0.98}Sc_{0.02}O_3$ with the orthorhombic lattice of Pnma was revealed. And the change of diffraction peaks $YFe_{0.95}Sc_{0.05}O_3$ and $YFe_{0.90}Sc_{0.10}O_3$ were indexed well with the hexagonal structure which indicated the transformation of two $YFeO_3$ structures, and the main orthorhombic phase can also be detected. This showed Sc can be used as a transformer of $YFeO_3$ structures, so the orthorhombic phase can partially transfer to hexagonal
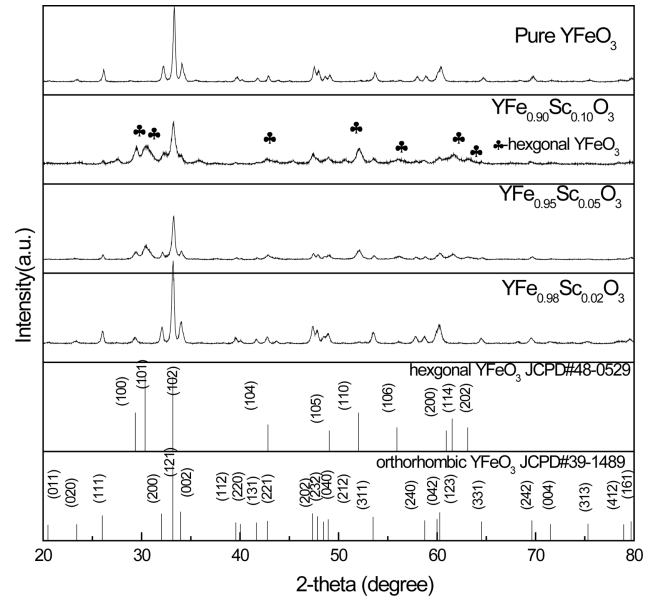
Fig. 1. The X-ray diffraction (XRD) patterns for as-prepared $YFe_{1-x}Sc_xO_3$ nanoparticles.

$YFeO_3$. As Sc^{+3} possesses a larger ionic radius of (0.885 Å) comparted with Fe^{+3} (0.738 Å), orthorhombic phase is not stable and can be changed as hexagonal phase.
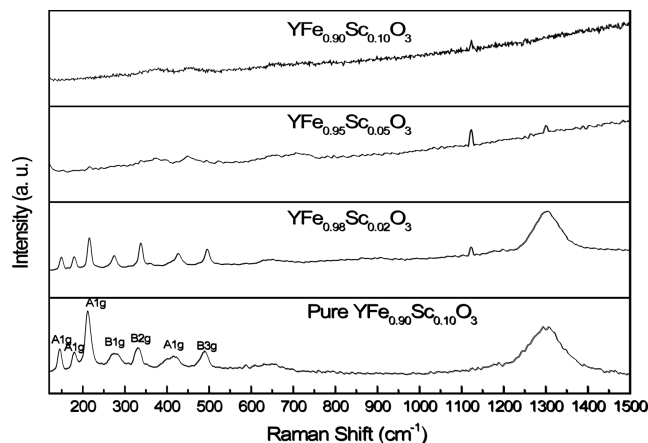
SEM images of Sc-doped nanoparticles are presented in
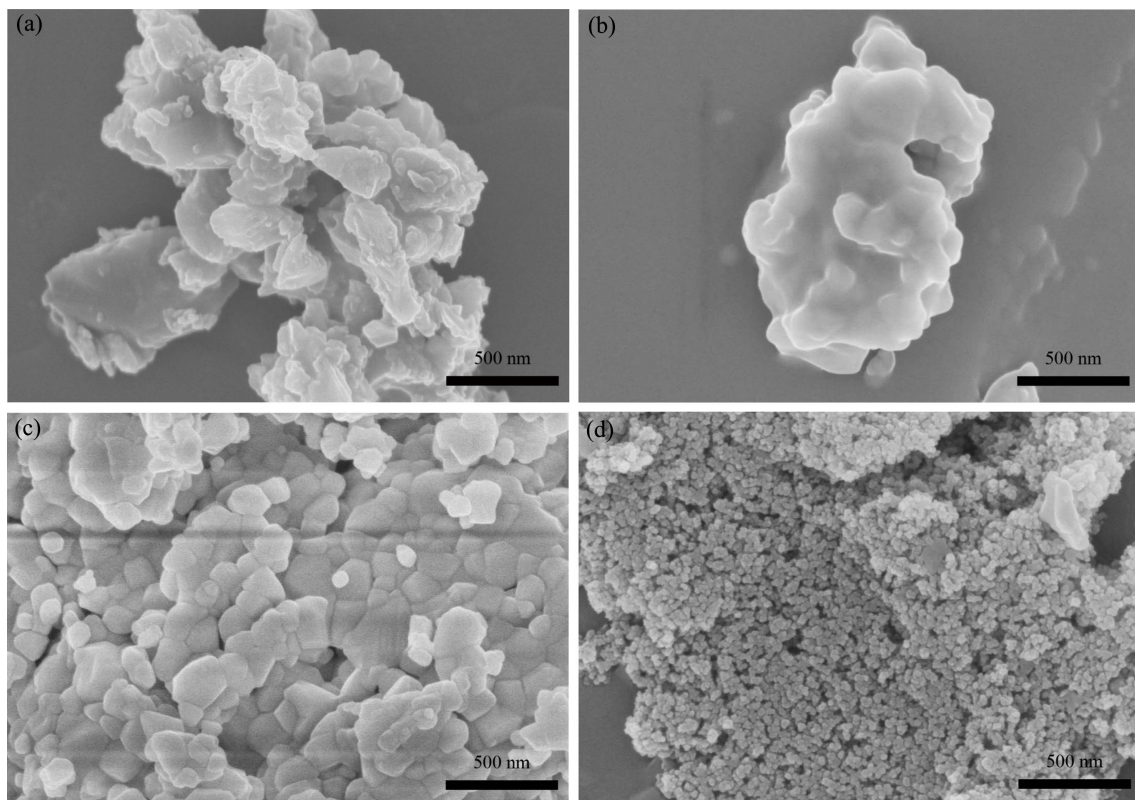
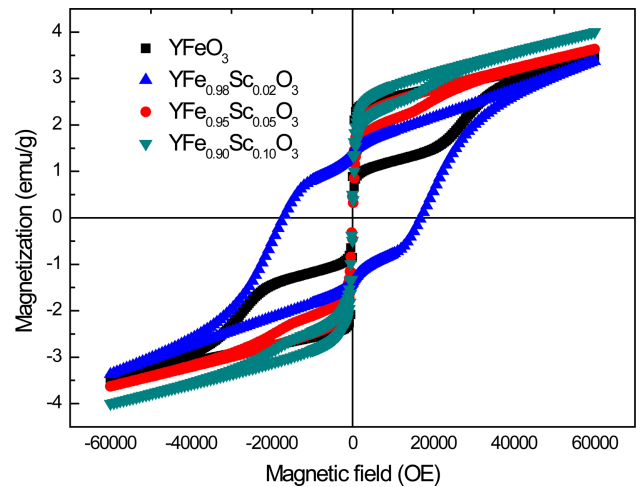**Fig. 2.** SEM micrographs of (a) $YFeO_3$, (b) $YFe_{0.98}Sc_{0.02}O_3$, (c) $YFe_{0.95}Sc_{0.05}O_3$, and (d) $YFe_{0.90}Sc_{0.10}O_3$.

Fig. 2, including homogeneous nanoparticles with minor agglomeration. The pristine $YFeO_3$ nanoparticles kept size at 400 nm. For $YFe_{0.98}Sc_{0.02}O_3$, $YFe_{0.95}Sc_{0.05}O_3$ and $YFe_{0.90}Sc_{0.10}O_3$, the sizes were approximately 300, 150, 50 nm, respectively, which were calculated by the area software from five images. The Sc^{3+} ions with a radius of (0.885 Å) was larger than Fe^{+3} (0.738 Å). The difference of lattice size led to some defects and strain, resulting in the refinement of particles. And hexagonal $YFeO_3$ particles are usually smaller than orthorhombic phase, which is related to smaller unit cell. These two factors lead to $YFeO_3$ particle refinement by Sc addition. The agglomeration of Sc-doped nanoparticles is reduced, given a large surface-volume ratio for nanoparticles, according to other references [13, 14]. It is proved that Sc can successfully change the morphology of $YFeO_3$ and reduce the size of particles.

Figure 3 shows the Raman spectra obtained from the $YFe_{0.98}Sc_{0.02}O_3$, $YFe_{0.95}Sc_{0.05}O_3$, and $YFe_{0.9}Sc_{0.1}O_3$ powders. For the perovskite structure $YFeO_3$, there are 60 optical phonon modes. It is known that some A_{1g} and B_g are active. The first two A_{1g} modes is connected to Y-O bonds, while other modes is associated with Fe-O bonds [15, 16]. The highest peak at 215 cm^{-1} is assigned to the octahedral of FeO_6. For $YFe_{0.98}Sc_{0.02}O_3$ particles, the first and second A_{1g} modes moved to higher frequency. Because Sc possesses a lower atomic weight than that of Fe, it illustrates that the Sc successfully substitutes Fe in $YFeO_3$. Moreover, the peaks are turning a little boarder since the doping of Sc introduce lattice disorder. For $YFe_{0.95}Sc_{0.05}O_3$ and $YFe_{0.90}Sc_{0.10}O_3$ particles, the additional peaks of Y-O bond represent the hexagonal $YFeO_3$, in consistence with the literature [15, 16], and the peak for orthorhombic perovskite structure is becoming weak. The highest peak at 1300 cm^{-1} ascribed to magnetic divalent Fe ions, which

Fig. 4. (Color online) Magnetic hysteresis loops of the $YFe_{1-x}Sc_xO_3$ nanoparticle.

is in accordance with those reported in $YFeO_3$ ceramics [17-19]. And this is totally disappeared in the $YFe_{0.95}Sc_{0.05}O_3$ and $YFe_{0.90}Sc_{0.10}O_3$ particles. So the phase is partially changed from orthorhombic perovskite phase to hexagonal one.

Figure 4 shows magnetic hysteresis loops of $YSc_xFe_{1-x}O_3$ nanoparticles. The maximum magnetization (M_m), remnant magnetization (M_r) and coercive field (H_c) of the pure $YFeO_3$ powders were 3.49 emu/g, 0.88 emu/g and 160 Oe, respectively. And the values were around 3.35emu/g, 1.41 emu/g and 17000 Oe for the $YFe_{0.98}Sc_{0.02}O_3$ powders and around 3.63 emu/g, 0.46 emu/g and 100 Oe for the $YFe_{0.95}Sc_{0.05}O_3$ powders. The values were around 4.00 emu/g, 0.53 emu/g and 120 Oe for the $YFe_{0.90}Sc_{0.10}O_3$ powders (Table 1). The shape of magnetic hysteresis loops was typically antiferromagnetic with weak magnetic materials, and the sudden increase of coercive field of $YFe_{0.98}Sc_{0.02}O_3$ was possibly caused by some minor impurities. It is well known that $YFeO_3$ is antiferromagnetic and presents weak magnetic properties. The reason for improving the maximum magnetization is the nano-effect of refined particles caused by Sc addition. And the hexagonal $YFeO_3$ is paramagnetic, and this can

Fig. 3. Raman spectra for as-prepared $YFe_{1-x}Sc_xO_3$ nanoparticles.

Table 1. List of the magnetic and optical parameters for $YFe_{1-x}Sc_xO_3$ nanopowders calcined.

Sample	M_m (emu/g)	M_r (emu/g)	H_c (kOe)	Photon energy (eV)
$YFeO_3$	3.49	0.88	160	2.42
$YFe_{0.98}Sc_{0.02}O_3$	3.35	1.41	17000	2.32
$YFe_{0.95}Sc_{0.05}O_3$	3.63	0.46	100	2.22
$YFe_{0.90}Sc_{0.10}O_3$	4.00	0.53	120	2.20
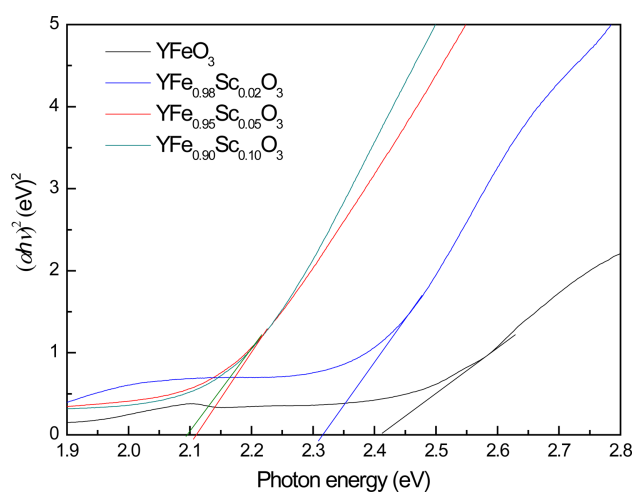
Fig. 5. (Color online) $(\alpha h\nu)^2$ as a function of photon energy for as-prepared nanoparticles.

reduce remnant magnetization (M_r) and coercive field (H_c) of $YFeO_3$ so as to generally result in better magnetic properties.

$YFeO_3$ possesses a narrow optical band gap and has been used as a light photocatalyst. According to the UV-visible absorption spectra, the optical energy band gap (E_g) of these samples can be calculated by Eq. (1) [20]:

$$(\alpha h\nu)^n = A(h\nu - E_g) \qquad (1)$$

$(\alpha h\nu)^2$ verses photon energy plots of $YFe_{0.98}Sc_{0.02}O_3$, $YFe_{0.95}Sc_{0.05}O_3$, and $YFe_{0.90}Sc_{0.10}O_3$ are shown in Fig. 5. The E_g values were 2.42, 2.32, 2.22, 2.20 for the $YFeO_3$, $Fe_{0.98}Sc_{0.02}O_3$, $YFe_{0.95}Sc_{0.05}O_3$, and $YFe_{0.90}Sc_{0.10}O_3$ nanoparticles (Table 1). The decrease of E_g of Sc-doped $YFeO_3$ was mainly due to the formation of hexagonal $YFeO_3$ [6]. The hexagonal $YFeO_3$ showed better optical property, because the narrow optical band gap of hexagonal $YFeO_3$ led to more effective visible-light absorption. Another reason was that the energy band gap decreased in line with the reduced powder size due to the nano-size effect, which induced more optical absorbance. Therefore, the Sc-doped $YFeO_3$ nanoparticles were considered a good candidate for decomposition of organic compounds.

4. Conclusion

Sc-doped $YFeO_3$ nanoparticles were successfully fabricated by low-temperature solid-state reaction, and a transition from orthorhombic to hexagonal with Sc addition was verified. The refined nanoparticles with ~50 nm size can be obtained. The maximum magnetization of Sc-doped $YFeO_3$ powders was about 4.00 emu/g. The energy band gap of $YFeO_3$ nanoparticles was reduced from 2.42 to 2.20 with increasing Sc concentration, which indicated their promising decomposition application. This method is easy to be adopted to fabricate and adjust $YFeO_3$.

References

[1] E. Salje, Ferroelectrics **104**, 111 (1990).

[2] G. Smolenskiĭ and I. Chupis, Soviet Physics Uspekhi **25**, 475 (1982).

[3] N. A. Hill, ACS Publications, 2000.

[4] S.-W. Cheong and M. Mostovoy, Nature Materials **6**, 13 (2007).

[5] T. Kimura, T. Goto, H. Shintani, K. Ishizaka, T. Arima, and Y. Tokura, Nature **426**, 55 (2003).

[6] M. Wang, T. Wang, S. Song, Q. Ma, and R. Liu, Materials **10**, 267 (2017).

[7] Y. Lu, S. Keav, V. Marchionni, G. L. Chiarello, A. Pappacena, M. Di Michiel, M. A. Newton, A. Weidenkaff, and D. Ferri, Catalysis Science & Technology **4**, 2919 (2014).

[8] M. Shang, C. Zhang, T. Zhang, L. Yuan, L. Ge, H. Yuan, and S. Feng, Appl. Phys. Lett. **102**, 062903 (2013).

[9] M. Sharon and B. M. Prasad, Electrochim. Acta **30**, 331 (1985).

[10] P. Tang, H. Chen, F. Cao, and G. Pan, Catal. Sci. Technol. **1**, 1145 (2011).

[11] M. A. Butler, D. S. Ginley, and M. Eibschutz, J. Appl. Phys. **48**, 3070 (1977).

[12] S. Shannigrahi, A. Huang, N. Chandrasekhar, D. Tripathy, and A. Adeyeye, Appl. Phys. Lett. **90**, 022901 (2007).

[13] D. Du Boulay, E. N. Maslen, V. A. Streltsov, and N. Ishizawa, Acta Crystallogr. Sect. B: Struct. Sci. **51**, 921 (1995).

[14] S. Venugopalan and M. M. Becker, J. Chem. Phys. **93**, 3833 (1990).

[15] A. P. Kuzmenko, P. V. Abakumov, and M. B. Dobromyslov, J. Magn. Magn. Mater. **324**, 1262 (2012).

[16] L. Wu, J. C. Yu, L. Zhang, X. Wang, and S. Li, J. Solid State Chem. **177**, 3666 (2004).

[17] Y. Ma, X. M. Chen, and Y. Q. Lin, J. Appl. Phys. **103**, 124111 (2008).

[18] D. S. Schmool, N. Keller, M. Guyot, R. Krishnan, and M. Tessier, J. Appl. Phys. **86**, 5712 (1999).

[19] M. Shang, C. Wang, Y. Chen, F. Sun, and H. Yuan, Mater. Lett. **175**, 23 (2016).

[20] F. Gao, X. Y. Chen, K. B. Yin, S. Dong, Z. F. Ren, F. Yuan, T. Yu, Z. G. Zou, and J. M. Liu, Adv. Mater. **19**, 2889 (2007).